NEUTRON-STAR MERGERS AND NUCLEAR PHYSICS*

Andreas Bauswein[a], Ricard Ardevol Pulpillo[b]
James A. Clark[c], Oliver Just[b], Stephane Goriely[d]
Hans-Thomas Janka[b], Nikolaos Stergioulas[e]

[a]Heidelberg Institute for Theoretical Studies, Heidelberg, Germany
[b]Max Planck Institute for Astrophysics, Garching, Germany
[c]Georgia Institute of Technology, Atlanta, USA
[d]Université Libre de Bruxelles, Brussels, Belgium
[e]Aristotle University of Thessaloniki, Thessaloniki, Greece

(Received December 14, 2016)

Neutron-star mergers are closely related to nuclear physics. The nuclear equation of state determines the properties of neutron-star matter and sensitively affects the dynamics of the merger. Consequently, the gravitational-wave signal carries a strong imprint of the equation of state. This, in turn, offers the possibilities to infer incompletely known properties of high-density matter from observations of gravitational waves emitted by the neutron-star mergers. For instance, the frequency of the dominant post-merger oscillation mode is strongly affected by the stiffness of nuclear matter. Furthermore, unbound matter from the neutron-star mergers provides generally favorable conditions for the formation of heavy elements through the rapid neutron-capture process. The element formation is investigated by nuclear network calculations. The amounts of ejecta are influenced by the high-density equation of state, which also implies an impact on the properties of nuclear powered electromagnetic counterparts.

DOI:10.5506/APhysPolB.48.651

1. Introduction

After Advanced LIGO's first detection of gravitational waves from merging black-hole binaries, the observation of gravitational waves from a neutron-star merger is expected any time. In both types of systems, the merging

* Presented at the Zakopane Conference on Nuclear Physics "Extremes of the Nuclear Landscape", Zakopane, Poland, August 28–September 4, 2016.

is an inevitable consequence of the continuous gravitational-wave emission, which extracts energy from the binary and leads to a shrinking of the orbital separation. Current estimates of the neutron-star merger rate predict between 2 and 200 detections per year when the network of ground-based gravitational-wave instruments reaches its design sensitivity [1, 2].

In the very late phase prior to merging, the orbital period of a neutron-star binary is of the order of a millisecond. The two stars thus merge with a substantial fraction of the speed of light. The coalescence proceeds with a relatively high impact parameter (see *e.g.* [3] for a review). The outcome of the merging depends sensitively on the total binary mass. For high total binary masses, the merger remnant cannot be supported against gravitational collapse, and the central object forms a black hole on a dynamical time scale, while some material with high angular momentum forms an accretion torus around the central black hole. For lower total binary masses, the two merging stars form a single massive central neutron star. Because of the high angular momentum in the system, the central object is rapidly rotating and can be supported against the gravitational collapse even if the total mass exceeds the maximum mass of non-rotating neutron stars. The violent collision leads to shock heating and the temperature can reach several 10 MeV. Moreover, strong oscillations of the merger remnant are excited. Considering the observed distribution of masses in known neutron-star binaries, the most likely outcome of a merger is the formation of a hot, rotating, massive neutron-star remnant [4].

Two aspects of neutron-star mergers touch nuclear physics. *(i)* The dynamics of neutron-star mergers are sensitively affected by the incompletely known equation of state (EoS) of nuclear matter. Since the gravitational-wave emission is shaped by the bulk motion of matter, the signal also depends on the EoS. This, in turn, offers the possibility to infer properties of the EoS from detecting gravitational waves of a neutron-star merger. We will discuss this prospect in Sect. 2. *(ii)* Small amounts of matter become gravitationally unbound during the dynamical merger phase. These ejecta provide generally favorable conditions for the rapid neutron-capture process (r-process). The astrophysical production site producing heavy r-process elements is still not unambiguously identified. We will discuss neutron-star mergers as site of the r-process in Sect. 3.

It is worthwhile stressing that current knowledge about neutron-star mergers relies nearly exclusively on numerical calculations. By linking the observables to the underlying physical questions, these models are crucial to allow the interpretation of future measurements.

2. Gravitational waves and the equation of state of high-density matter

A typical gravitational-wave signal is shown in Fig. 1. The first ~ 7 milliseconds show the very last phase of the so-called inspiral with an increasing frequency and an increasing amplitude. The gravitational-wave signal during the inspiral is dominated by the orbital motion. The chirp-like signal is a result of the increasingly faster decay of the orbital separation. Importantly, the component masses of the binary can be measured from this inspiral phase because the masses are essentially determining the orbital motion. The two stars touch at about 7 ms. The gravitational-wave signal of the following

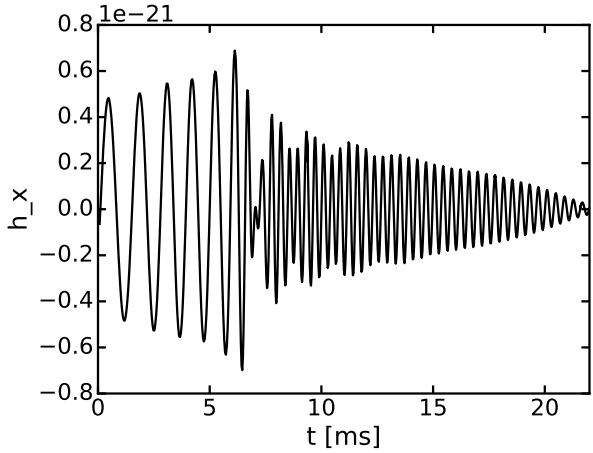

Fig. 1. Gravitational-wave amplitude (dimensionless) of a neutron-star merger at a distance of 20 Mpc (cross polarization). The initial phase shows the so-called inspiral up to about 7 ms followed by the characteristic oscillations of the postmerger phase.

postmerger phase is characterized by a dominant oscillation. This dominant oscillation is clearly visible as a pronounced peak in the kHz range of the gravitational-wave spectrum as shown in Fig. 2. Apart from the dominant peak, labeled f_{peak}, there are several other features in the spectrum which are clearly originating from the postmerger phase.

One can distinguish two basic effects of the EoS on the gravitational-wave signal of a neutron-star merger. By measuring these effects, information on the nuclear EoS can be inferred. *(i)* During the very late inspiral phase finite-size effects influence the orbital dynamics. Larger neutron stars lead to an accelerated inspiral and an earlier merging, *e.g.* [6]. *(ii)* The EoS affects the compactness of the merger remnant and thus its oscillation frequencies [7]. Stiffer EoSs lead to larger remnants, which oscillate at lower frequencies.

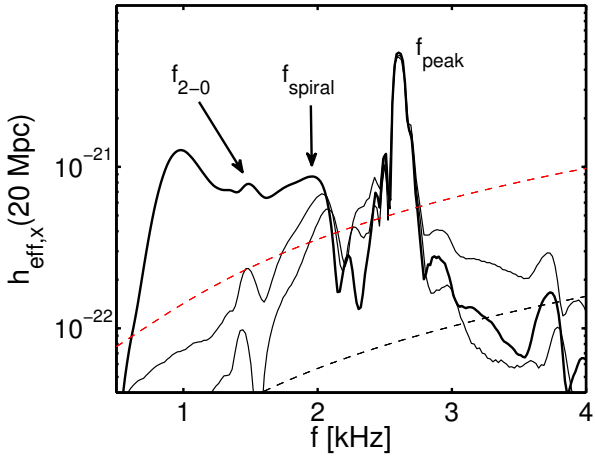

Fig. 2. Gravitational-wave spectrum of a neutron-star merger. Thin lines show the spectrum of only the postmerger phase. Various features can be identified in the spectrum, most notably the dominant postmerger oscillation at a frequency $f_{\rm peak}$. f_{2-0} is generated by a coupling between the quasi-radial oscillation of the remnant and the quadrupolar fluid mode (at $f_{\rm peak}$). $f_{\rm spiral}$ arises from the orbital motion of bulges at the outer remnant. Figure adapted from [5].

The dominant peak in the postmerger spectrum is generated by the fundamental quadrupolar fluid mode [8, 9]. Thus, one suspects that the dominant oscillation frequency scales with the size of the remnant, which has been shown in [7]. It has been found empirically that the dominant oscillation frequency of the postmerger phase also correlates with the radii of non-rotating neutron stars [7, 10]. This empirical relation is important because the mass-radius relation of non-rotating neutron stars is uniquely determined by the incompletely known EoS. Figure 3 exhibits the tight correlation between the dominant oscillation frequency and the radii of non-rotating neutron stars. A measurement of $f_{\rm peak}$ can thus be employed to determine the radius of a non-rotating neutron star, simply by inverting the empirical relation.

The feasibility of measuring the dominant postmerger oscillation frequency has been shown by simulated gravitational-wave searches [11, 12]. In theses studies, waveform models were randomly injected in a recorded data stream of a gravitational-wave detector — so basically hidden in realistic noise. Dedicated data analysis methods recovered the dominant frequency with very high precision employing either an unmodeled search or a principle component analysis.

Figure 3 shows data for a fixed binary setup (1.35–1.35 $M_\odot$ binaries). Relations between $f_{\rm peak}$ and neutron star radii can be found for other binary masses as well, see [7, 9, 13–16]. In this context, it is important to note that the inspiral gravitational-wave signal will reveal the masses of the binary components, *e.g.* [18]. We stress that a single detection of only the dominant postmerger frequency at $f_{\rm peak}$ is sufficient for a precise neutron-star radius measurement. Finally, we note that the postmerger gravitational-wave signal has the potential to uncover other unknown properties of neutron stars and the EoS, for instance the maximum mass of non-rotating neutron stars [9, 14].

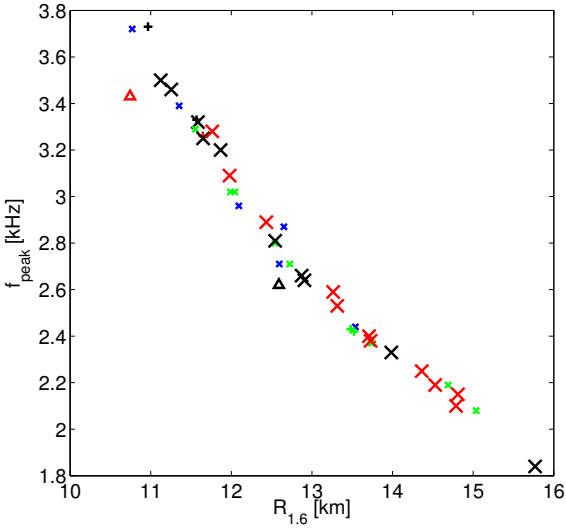

Fig. 3. (Color online) Relation between the dominant postmerger gravitational-wave frequency and the radius of non-rotating neutron stars for different candidate EoSs. Each EoS is characterized by the radius $R_{1.6}$ of a non-rotating neutron star with 1.6 $M_\odot$. Radii of non-rotating neutron stars are uniquely determined by the EoS. Results are shown for fixed binary masses, specifically 1.35–1.35 $M_\odot$ mergers. Binary masses can be measured from the inspiral phase. The triangles correspond to EoSs describing absolutely stable strange quark matter. Gray/red big crosses correspond to fully temperature-dependent EoSs. Other colors refer to EoS models at zero temperature, which are supplemented by an approximate treatment of thermal effects, see [17]. Black symbols show results for tabulated microphysical, cold EoSs. Dark gray/blue small crosses show results for EoS models within chiral effective field theory. Light gray/green small crosses display results for microphysical, cold EoSs which are described by a piecewise polytropic fit. Plus signs correspond to EoS models which are ruled out by the observation of neutron stars with gravitational masses of about 2 $M_\odot$. Figure adapted from [7], where more details can be found.

3. Neutron-star merger ejecta and the r-process

During the dynamical merger process, small amount of matter become gravitationally unbound. Typical ejecta masses are between 10^{-3} $M_\odot$ and 10^{-2} $M_\odot$ [19]. Originating mostly from the inner crust, this material is neutron-rich. Typical outflow velocities reach several tens per cent of the speed of light. Because of the very fast expansion, the ejecta provides generally favorable conditions for the r-process. Based on hydrodynamical merger simulations and nuclear network calculations, several studies showed that the resulting abundance distribution in the outflow follows closely the rescaled observed solar distribution [20–22]. It should be explored in more detail to which extent weak interactions drive the outflows less neutron-rich, which results in a production of more lighter nuclei compared to heavy r-process elements [23, 24].

It is worth noting that most of the ejecta originates from the contact interface between the colliding neutron stars [21]. Only for strongly asymmetric binary systems, a substantial amount of matter is ejected from a pronounced tidal tail. The origin from the contact interface explains the

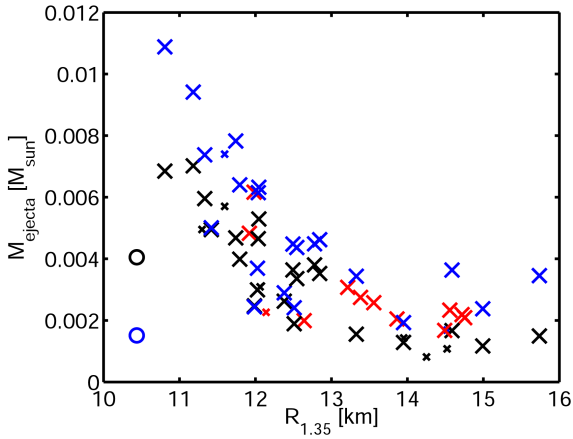

Fig. 4. Ejecta masses of 1.35–1.35 $M_\odot$ mergers for different EoSs characterized by the radius of a 1.35 $M_\odot$ neutron star. Soft EoSs (small neutron star radii) lead to more ejecta. $M_{\rm ejecta}$ refers to matter which is dynamically ejected within the first $\sim$ 10 ms after merging. Gray/red symbols refer to EoS models which provide the full temperature dependence. Light gray/blue and black symbols show results for EoS models which are based on cold barotropic EoSs supplemented with an approximate treatment of thermal effects [17]. Light gray/blue and black symbols show results from simulations which make different assumptions about the approximate inclusion of thermal effects. Figure taken from [19].

dependence of the ejecta mass on the nuclear EoS employed for describing high-density neutron-star matter. Soft EoSs result in more compact neutron stars. More compact neutron stars collide with a higher impact velocity, and thus the more violent merging squeezes out more ejecta [19]. This dependence is illustrated in Fig. 4 showing ejecta masses for 1.35–1.35 $M_\odot$ binary mergers with different EoSs. As in Fig. 3, different EoSs are characterized by the radii of a non-rotating neutron stars. One clearly recognizes the increase of the ejecta mass with the EoS softness. The reduced ejecta mass for very compact neutron stars is a result of the prompt collapse of the merger remnant.

The dependence of the ejecta mass on the EoS has implications for the properties of electromagnetic counterparts [25]. These transients are powered by nuclear decays during the r-process and typically reach their peak brightness on the time scale of days. The peak luminosity and peak time scale depend, for instance, on the ejecta mass and the outflow velocity. Thus, the properties of the light curves of the electromagnetic counterparts are affected by the EoS [19].

4. Rate estimates and nucleosynthesis

Determining the ejecta masses of compact object mergers (neutron star-neutron star mergers and neutron star-black hole mergers) can be employed for an independent estimate of the merger rate. The rate of compact object mergers is not very well-known and typically derived from population synthesis studies or from the observed sample of neutron-star binaries. Because of the uncertainties in these estimates, the exact detection rate of gravitational-wave detectors is still unknown. See, for instance, [1] for a compilation of different studies.

An independent estimate of the rate can be obtained by considering the observed amount of heavy r-process elements in the Galaxy, which can be inferred from the solar abundance and the baryonic mass of the Galaxy [26]. Under the assumption that most of the heavy r-process elements are produced by compact object mergers, a rate can be derived for a given average ejecta mass. Since neutron star-black hole mergers also produce heavy r-process elements, *e.g.* [27], one cannot discern this type of merger from neutron-star mergers. The estimate thus provides combinations of the rates of these two types of merger events. The colored bands in Fig. 5 show rates estimated with the described procedure. Different colors refer to different nuclear EoSs, which affect the average ejecta mass as detailed in Sect. 3 for neutron-star mergers. The bands have a finite width because the initial spin in neutron star-black hole mergers is not very well-constrained but strongly affects the average ejecta mass in this type of event.

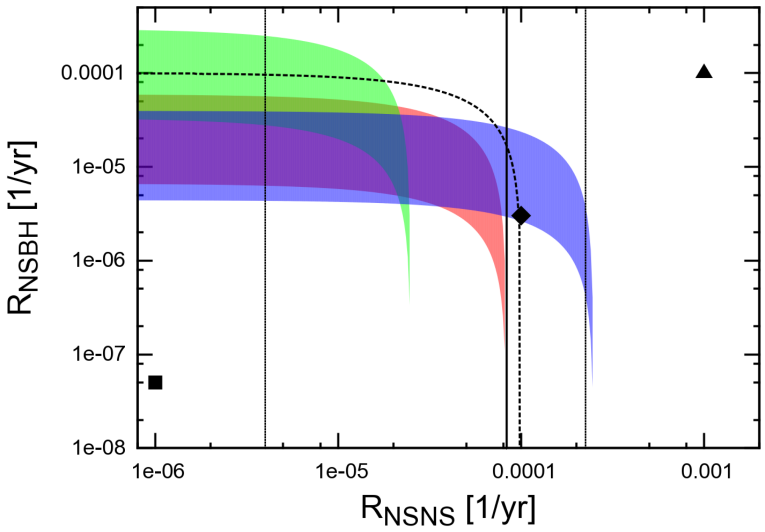

Fig. 5. (Color online) Merger rate of neutron star-black hole binaries as a function of merger rate of neutron-star binaries estimated from the Galactic content of heavy r-process elements. Different colors refer to different EoSs: dark gray/blue band for stiff neutron-star matter, gray/red for moderately stiff neutron-star matter, light gray/green for soft neutron-star matter. Symbols are rates estimates compiled in [1]. Figure taken from [26].

Given all the uncertainties of this estimate, Fig. 5 provides only the order of magnitude of the different rates. But interestingly, the data are compatible with the rate estimates from [1] which have been classified as "realistic" (diamond in Fig. 5). Based on the rate estimate via nucleosynthesis, the "optimistic" rate from [1] (triangle) is ruled out, otherwise one would observe more heavy r-process elements in the Galaxy. Overall, the estimate based on the Galactic r-process element content corroborates the expectation that the first detections of neutron-star mergers will succeed with the current generation of ground-based instruments as they approach their design sensitivity.

Support by the Klaus-Tschira Foundation is acknowledged. We acknowledge partial support by the Deutsche Forschungsgemeinschaft through Excellence Cluster 'Universe' EXC-153.

REFERENCES

[1] J. Abadie *et al.*, *Class. Quantum Grav.* **27**, 173001 (2010).

[2] B.P. Abbott *et al.*, *Living Rev. Relativ.* **19**, 1 (2016).

[3] J.A. Faber, F.A. Rasio, *Living Rev. Relativ.* **15**, 8 (2012).

[4] A. Bauswein, T.W. Baumgarte, H.-T. Janka, *Phys. Rev. Lett.* **111**, 131101 (2013).

[5] A. Bauswein, N. Stergioulas, *Phys. Rev. D* **91**, 124056 (2015).

[6] J.S. Read *et al.*, *Phys. Rev. D* **88**, 044042 (2013).

[7] A. Bauswein, H.-T. Janka, K. Hebeler, A. Schwenk, *Phys. Rev. D* **86**, 063001 (2012).

[8] N. Stergioulas, A. Bauswein, K. Zagkouris, H.-T. Janka, *Mon. Not. R. Astron. Soc.* **418**, 427 (2011).

[9] A. Bauswein, N. Stergioulas, H.-T. Janka, *Eur. Phys. J. A* **52**, 56 (2016).

[10] A. Bauswein, H.-T. Janka, *Phys. Rev. Lett.* **108**, 011101 (2012).

[11] J.A. Clark *et al.*, *Phys. Rev. D* **90**, 062004 (2014).

[12] J.A. Clark, A. Bauswein, N. Stergioulas, D. Shoemaker, *Class. Quantum Grav.* **33**, 085003 (2016).

[13] K. Hotokezaka *et al.*, *Phys. Rev. D* **88**, 044026 (2013).

[14] A. Bauswein, N. Stergioulas, H.-T. Janka, *Phys. Rev. D* **90**, 023002 (2014).

[15] S. Bernuzzi, T. Dietrich, A. Nagar, *Phys. Rev. Lett.* **115**, 091101 (2015).

[16] K. Takami, L. Rezzolla, L. Baiotti, *Phys. Rev. D* **91**, 064001 (2015).

[17] A. Bauswein, H.-T. Janka, R. Oechslin, *Phys. Rev. D* **82**, 084043 (2010).

[18] C.L. Rodriguez *et al.*, *Astrophys. J.* **784**, 119 (2014).

[19] A. Bauswein, S. Goriely, H.-T. Janka, *Astrophys. J.* **773**, 78 (2013).

[20] C. Freiburghaus, S. Rosswog, F.-K. Thielemann, *Astrophys. J. Lett.* **525**, L121 (1999).

[21] S. Goriely, A. Bauswein, H.-T. Janka, *Astrophys. J. Lett.* **738**, L32 (2011).

[22] J. d. Jesús Mendoza-Temis *et al.*, *Phys. Rev. C* **92**, 055805 (2015).

[23] S. Wanajo *et al.*, *Astrophys. J. Lett.* **789**, L39 (2014).

[24] S. Goriely *et al.*, *Mon. Not. R. Astron. Soc.* **452**, 3894 (2015).

[25] B.D. Metzger *et al.*, *Mon. Not. R. Astron. Soc.* **406**, 2650 (2010).

[26] A. Bauswein, R. Ardevol Pulpillo, H.-T. Janka, S. Goriely, *Astrophys. J. Lett.* **795**, L9 (2014).

[27] O. Just *et al.*, *Mon. Not. R. Astron. Soc.* **448**, 541 (2015).